Scientific Research Publishing

Open Journal of Composite Materials, 2017, 7, 130-145
http://www.scirp.org/journal/ojcm
ISSN Online: 2164-5655
ISSN Print: 2164-5612

On the s±-Wave Superconductivity in the Iron-Based Superconductors: A Perspective Based on a Detailed Study of $Ba_{0.6}K_{0.4}Fe_2As_2$ via the Generalized-Bardeen-Cooper-Schrieffer Equations Incorporating Fermi Energy

G. P. Malik[1,2]

[1]School of Environmental Sciences, Jawaharlal Nehru University, New Delhi, India
[2]Present Address: B-208 Sushant Lok 1, Gurgaon 122009, Haryana, India
Email: gulshanpmalik@yahoo.com, malik@mail.jnu.ac.in

How to cite this paper: Malik, G.P. (2017) On the s±-Wave Superconductivity in the Iron-Based Superconductors: A Perspective Based on a Detailed Study of $Ba_{0.6}K_{0.4}Fe_2As_2$ via the Generalized-Bardeen-Cooper-Schrieffer Equations Incorporating Fermi Energy. *Open Journal of Composite Materials*, **7**, 130-145.
https://doi.org/10.4236/ojcm.2017.73008

Received: June 6, 2017
Accepted: July 4, 2017
Published: July 7, 2017

Abstract

Guided by the belief that Fermi energy E_F (equivalently, chemical potential μ) plays a pivotal role in determining the properties of superconductors (SCs), we have recently derived μ-incorporated Generalized-Bardeen-Cooper-Schrieffer equations (GBCSEs) for the gaps (Δs) and critical temperatures (T_cs) of both elemental and composite SCs. The μ-dependent interaction parameters consistent with the values of Δs and T_cs of any of these SCs were shown to lead to expressions for the effective mass of electrons (m^*) and their number density (n_s), critical velocity (v_0), and the critical current density j_0 at T = 0 in terms of the following five parameters: Debye temperature, E_F, a dimensionless construct y, the specific heat constant, and the gram-atomic volume. We could then fix the value of μ in any SC by appealing to the experimental value of its j_0 and calculate the other parameters. This approach was followed for a variety of SCs—elemental, MgB_2 and cuprates and, with a more accurate equation to determine y, for Nitrogen Nitride (NbN). Employing the framework given for NbN, we present here a detailed study of $Ba_{0.6}K_{0.4}Fe_2As_2$ (BaAs). Some of the main attributes of this SC are: it is characterized by $s^{\pm}$-wave superconductivity and multiple gaps between 0 - 12 meV; its $T_c \sim 37$ K, but the maximum T_c of SCs in its class can exceed 50 K; $E_F/kT_c = 4.4$ (k = Boltzmann constant), and its T_c plotted against a tuning variable has a dome-like structure. After drawing attention to the fact that the $s^{\pm}$-wave is an inbuilt feature of GBCSEs, we give a quantitative account of its several other features, which include the values of m^*, n_s, v_o, and coherence length. Finally, we also deal with the issue of the stage BaAs occupies in the BCS-Bose-Einstein Condensation crossover.

Keywords

Iron-Based Superconductors, Multiple Gaps, T_cs, and Other Properties of $Ba_{0.6}K_{0.4}Fe_2As_2$, GBCSEs, Fermi energy, BCS-BEC Crossover

1. Introduction

Ever since their discovery in 2008 by Kamihara *et al.* [1], the iron-based superconductors (FeSCs) characterized by multiple gaps (Δs) and high-T_cs have been avidly investigated both experimentally and theoretically. This is evidenced by at least *ten* review articles in a relatively short period, as has been noted in another, more recent, review by Bang and Stewart [2]. While the issue of the pairing mechanism in FeSCs remains an open question, the conventional theoretical approaches proposed to deal with them have been broadly categorized in [2] as based on the Random Phase Approximation, the Functional Renormalization Group Technique, and the Local Pairing Approach. A common feature of these is their adaptations of the multi-band concept, which was pioneered by Suhl *et al.* [3]. We propose in this note to show that many properties of FeSCs are also explicable quantitatively via another approach which is based on a generalization of the one-band Bardeen-Cooper-Schrieffer equations (GBCSEs) in the mean-field approximation.

Since such a proposal may *prima facie* seem as bizarre, there seems a need at the outset to make it physically plausible that the approach based on GBCSEs may, at least, play a valuable role in supplementing the conventional multi-band approach. This need is addressed in Section 2, where (a) the genesis of employing the multi-band approach for high-T_c SCs is outlined and (b) the physical content of GBCSEs is summarized. For the sake of concreteness, we apply GBCSEs here to the most widely investigated FeSC, *i.e.*, $Ba_{0.6}K_{0.4}Fe_2As_2$ (BaAs hereafter). Listed in Section 3 therefore are its main properties, which are based on various experiments and the conventional theoretical approaches. The study of BaAs via GBCSEs incorporating chemical potential μ (equivalently Fermi energy E_F, as will be discussed below) is taken up in Section 4 and is shown to lead to the important result that E_F characterizing it is ~14 meV. In Section 5 we show how this result enables us to shed light on the properties of the SC that were noted in Section 3, Sections 6 and 7 are devoted, respectively, to a Discussion and Conclusions of our approach.

2. Multi-Band Models and GBCEs

Because SCs characterized by multiple gaps are most commonly addressed by invoking multi-band models, with an apology to the cognoscenti, we first trace below the backdrop of these models. This is followed up by an account of the physical considerations that led to GBCSEs.

Iron-based superconductors.

2.1. The Multi-Band Models

The conceptual basis for multi-band models in general is provided by Suhl *et al.* [3] who dealt with the superconductivity of transition elements. A peculiar feature of these elements is the filling up of the 4s orbital prior to the 3d orbital, which implies that the valence electrons in these elements are divided between two bands. Therefore, the s-electrons can be scattered not only within their own band, but also to the d-band. Because the latter band has more vacant levels than the former, it makes a large contribution to the total density of states $N(0)$. Two gaps and, in general, two T_cs arise in this approach because the BCS interaction parameter $\lambda \equiv [N(0)V]$ is now determined via a quadratic equation involving interaction energies V between pairs of electrons in the two bands individually and those that are scattered from one band to the other. It is to be noted that in this model the equation employed to determine T_c– for each value of λ – is identical with the equation that determines this parameter in the original, one-band BCS equation. Since the latter equation has been shown to follow from a Bethe-Salpeter equation (BSE) in the scenario of one-phonon exchanges between Cooper pairs (CPs) [4] [5], and since this approach must satisfy the Bogoliubov constraint, *i.e.* $\lambda \leq 0.5$, it follows that it cannot, *per se*, account for such high-T_cs as have been observed. This of course is the reason why numerous attempts have been made to integrate the multi-band concept with the well-known Migdal-Eliashberg-McMillan approach [6]. The latter approach allows λ to be greater than unity because it is based on an integral equation the successive terms in which are smaller by a factor of (m_e/M), rather than λ; here m_e is the mass of an electron and M that of an ion. Since λ can now be greater than unity, it has been implied that the occurrence of high-T_cs is explicable via this approach. Note however that this is a surmise made by remaining in the conceptual mould where formation of CPs is brought about via one-phonon exchange mechanism (1PEM), ignoring the possibility that in a composite SC electrons may also be bound via simultaneous phonon exchanges with more than one species of ions—each of which is distinguished by its own Debye temperature and interaction parameter.

2.2. GBCSEs: Physical Basis

Superconductivity in *any* material has to-date been understood solely as arising due to the formation of CPs. In elemental SCs, pairing is brought about via 1PEM due to a net attraction between pairs of electrons because of the ion-lattice and the Coulomb repulsion.

No single-component SC has yet been found with a T_c exceeding that of Nb, *i.e.*, 9.25 K ($\Delta \approx 1.55$ meV). In the light of this observation, a general feature of SCs characterized by high-T_cs and multiple gaps is striking: *all* of them are multi-component materials. This naturally suggests that CPs in these may be bound via simultaneous exchanges of phonons with more than one species of ions – in addition to those that are bound via 1PEM due to each ion species separately. It has been shown that the BCS equation for the T_c of an elemental SC follows by summing an infinite number of ladder diagrams in the 1PEM scenario [4] [5].

The first diagram in this series has one step or rung, the second two rungs, and so on. If the number of rungs between any two space-time points in each of these diagrams is doubled, then we have the 2-phonon exchange mechanism (2PEM) in operation. Similarly, CPs may also be bound via the 3-phonon exchange mechanism (3PEM) if the SC contains three species of ions that can potentially cause formation of CPs. It then follows that in a multi-component SC, CPs may exist with different values of the binding energy (2|W|). Since the binding energy of CPs in the 3PEM scenario must be greater than in the 2PEM scenario, which in turn must be greater than in the 1PEM scenario, and since $|W| = \Delta$ [5], we are naturally led to an explanation of why multi-component SCs are characterized by multiple gaps. Equations for the $|W|$s and T_cs of composite SCs have been derived by invoking multiple-phonon exchange mechanism for pairing—which simply means that the one-phonon propagator in the BSE which leads to the BCS expression for the T_c of an elemental SC is replaced by a "superpropagator". Since the equations so obtained manifestly generalize the corresponding BCS equations for an elemental SC, they were christened as GBCSEs.

3. Properties of Superconducting BaAs

In the following Sections, we shall show how GBCSEs enable one to correlate several properties of BaAs and shed light on others. These properties are listed below; they include not only those that are determined via different experiments, viz., the angle-resolved photoemission spectroscopy (ARPES), the scanning tunnelling microscopy, and specific heat and penetration-depth measurements, but also those determined via theoretical investigations based on multi-band models and a study of the crossover from a BCS state to a Bose-Einstein Condensed state (crossover hereafter).

Properties of BaAs addressed in this note:

(i) Superconductivity in this SC is due to the $s^{\pm}$ - wave state, which signifies that the gaps below a Fermi surface and above it, Δ_h and Δ_e, respectively, have opposite signs [2];

(ii) In general, $|\Delta_h| \neq |\Delta_e|$ [2];

(iii) $T_c = 37$ K [7];

(iv) Maximum value of T_c for several FeSCs [8] [9]:

$$(T_c)_{\max} \succ 50 \text{ K};$$

(v) $\Delta_1, \Delta_2 = 6, 12$ meV [10];

(vi) Near-zero values of Δ: As reported in several papers, e.g., [11], Δ for the SC being considered can fall to zero along lines of the Fermi surface

(vii) Some of the other reported values of Δ (in meV): 2.5, 9.0 [12], 3.3, 7.6 [7], 3.6, 8.5, 9.2 [13]; 4, 7 12, 9.5 [14],

(viii) Crossover: It has been asserted that BaAs lies nearly in the middle of crossover regime [15] with Δ/E_F ratios as:

$$0.55 < \Delta_1/E_F < 1.3,$$

$$\Delta_2/E_{F_2} = 0.5 \quad (\Delta_2/\Delta_1 = 2.5).$$

The last equation is obtained via a two-band model for which the Fermi energies are defined as $E_{F_i} = \mu - \varepsilon_i \ (i = 1, 2)$ with $\varepsilon_1 = 0$ and tuneable $\varepsilon_2 \geq 0$;

(ix) The critical current density j_0: It has been reported as *exceeding* 0.1 MA cm^{-2} [16] at $T = 4.2$ K and $H = 0$ T (H being the external magnetic field) and as 1.1×10^7 Acm^{-2} [17] at 2 K and 0 T. Based on these experimental values we estimate j_0 for BaAs as $\approx 2.5 \times 10^7$ Acm^{-2} at $T = H = 0$;

(x) Another characteristic ratio, see, e.g., [9]: $E_F/kT_c = 4.4$;

(xi) The band effective mass m^* and the free electron mass m_e: In a study of BaAs based on ARPES and a four-band model, Ding *et al.* [18] have reported that in one of the bands, $s \equiv m^*/m_e = 9.0$ (other values are lower), and have estimated

(xii) The coherence length ξ as 9 - 14 Å; and finally,

(xiii) Dome-like structure: T_c of the SC plotted against a "tuning variable" has a dome-like structure [9].

4. Study of BaAs via GBCSEs

4.1. Equation for $|W|$ in the 1PEM Scenario and the BCS Equation for Δ

Prior to undertaking the study of BaAs via the multi-phonon exchange mechanism, we recall that the equation for $|W|$ at $T = 0$ in the 1PEM scenario ($E_F \gg k\theta$) is [5]:

$$|W| = \frac{2k\theta}{\exp(1/\lambda) - 1}.$$

For the sake of comparison, we also recall the BCS equation for Δ:

$$\Delta = \frac{k\theta}{\sinh(1/\lambda)},$$

which follows from an equation *quadratic* in Δ. Significantly, the equation for W has been derived by assuming that its sign changes in going from below the Fermi surface to above it, which is (a) akin to a similar change in the velocity of a quasi-particle, as discussed by Rickayzen [19], and (b) also the case for all the equations employed below. Hence from the outset our approach is based on the $s^{\pm}$ - wave feature noted as Property (i) above. It was shown in [20] via a detailed study of six elemental SCs that the above equation for $|W|$ is a viable alternative to the equation for Δ.

4.2. Debye Temperatures (θs) of the Constituents of BaAs

The first step in the application of GBCSEs to any composite SC is to identify the ion species that may cause pairing. For BaAs, we identify them as Ba, Fe and As. Given $\theta_{\mathrm{BaAs}} = 274$ K [21] and the masses of the ion-species, the next step is to fix θ_{Ba}, θ_{Fe}, and θ_{As}, which *must* be different because the masses of the ions are different. One way of doing this is to assume that the modes of vibration in any

layer of the SC simulate the modes of vibration of a double pendulum. For the layer containing Ba and K ions, for example, we are then led to two values for both θ_{Ba} and θ_{K}– one corresponding to Ba as the upper bob of the double pendulum and K as the lower bob and the other by interchanging the positions of the bobs. We are similarly led to two values for both θ_{Fe} and θ_{As}. While all these values have been given in [22], we adopt here the following set (this will be further discussed below):

$$\theta_{Ba} = 124.58 \text{ K}, \ \theta_{\mathrm{Fe}} = 399.43 \text{ K}, \ \theta_{\mathrm{As}} = 148.57 \text{ K} \ \left(\theta_{\mathrm{BaAs}} = 274 \text{ K}\right) \tag{1}$$

4.3. GBCSEs Sans μ

We first deal with the gaps and the T_c of BaAs via GBCSEs sans μ, which were obtained by assuming that E_F (or μ) $\gg k\theta$. The results so obtained will be seen to provide a consistency check of the μ-incorporated GBCSEs in the next section.

The features of BaAs that we take as our starting point are

$$\Delta_1 = |W_2| = 6 \text{ meV}, \ \Delta_2 = |W_3| = 12 \text{ meV}, \ T_c = 37 \text{ K}. \tag{2}$$

Since GBCSEs are based on the formation of CPs via multi-phonon exchange mechanisms, let us define W_1, W_2 and W_3 as the $T = 0$ values of (half) the binding energies of pairs formed via 1PEM, 2PEM and 3PEM, respectively. We now identify W_2 with the smaller and W_3 with the larger of the two gaps in the set of Equations (2) and the value of T_c as the temperature at which W_2 vanishes. While 2PEM can be caused by any combination of ions such as (Ba + As), (Fe + As), and (Ba + Fe), all of which were considered in [22], for the limited purpose of checking the consistency of equations in the next section, we now adopt the last of these options. Then, for E_F (or μ) $\gg k\theta_{\mathrm{BaAs}}$ we have the following set of equations [22] ($W_i = |W_i|$):

$$1 = \lambda_{\mathrm{Ba}} \ln\left[1 + \frac{2k\theta_{\mathrm{Ba}}}{W_2}\right] + \lambda_{\mathrm{Fe}} \ln\left[1 + \frac{2k\theta_{\mathrm{Fe}}}{W_2}\right] \tag{3}$$

$$1 = \lambda_{\mathrm{Ba}} \ln\left[1 + \frac{2k\theta_{\mathrm{Ba}}}{W_3}\right] + \lambda_{\mathrm{Fe}} \ln\left[1 + \frac{2k\theta_{\mathrm{Fe}}}{W_3}\right] + \lambda_{\mathrm{As}} \ln\left[1 + \frac{2k\theta_{\mathrm{As}}}{W_3}\right] \tag{4}$$

$$1 = \lambda_{\mathrm{Ba}} \int_0^{\theta_{\mathrm{Ba}}/2T_c} \mathrm{d}x \frac{\tanh(x)}{x} + \lambda_{\mathrm{Fe}} \int_0^{\theta_{\mathrm{Fe}}/2T_c} \mathrm{d}x \frac{\tanh(x)}{x} \tag{5}$$

Solutions of the above equations, with inputs from the sets of Equations (2) and (3), lead to $\{\lambda_{\mathrm{Ba}} = -0.0484, \lambda_{\mathrm{Fe}} = 0.4254$, and $\lambda_{\mathrm{As}} = 0.2084\}$. Since each value of λ must satisfy the Bogoliubov constraint ($0 < \lambda \leq 0.5$), this set of solutions in unacceptable. This situation is addressed by a minor fine-tuning of the input variables as discussed in detail in [23]. In the present instance, it turns out that solely changing $|W_2|$ from 6 to 6.2 meV leads to the following acceptable set

$$\{\lambda_{\mathrm{Ba}}, \lambda_{\mathrm{Fe}}, \lambda_{\mathrm{As}}\} = \{0.0308, 0.3826, 0.2084\}. \tag{6}$$

4.4. μ-Incorporated GBCSEs

Generalized versions of Equations (3)-(5) that do away with the constraint E_F (or μ) $\gg k\theta$ are [24]:

$$I_1^{(2)}\left(\theta_{\mathrm{Ba}},\theta_{\mathrm{Fe}},\mu,|W_2|\right)-\left[\frac{3}{4}I_2^{(2)}\left(\theta_{\mathrm{Fe}},\mu,|W_2|\right)\right]^{1/3}=0 \tag{7}$$

$$I_1^{(3)}\left(\theta_{\mathrm{Ba}},\theta_{\mathrm{Fe}},\theta_{\mathrm{As}},\mu,|W_3|\right)-\left[\frac{3}{4}I_2^{(3)}\left(\theta_{\mathrm{Fe}},\mu,|W_3|\right)\right]^{1/3}=0 \tag{8}$$

$$I_3^{(2)}\left(\theta_{\mathrm{Ba}},\theta_{\mathrm{Fe}},\mu,T_c\right)-\left[\frac{3}{4}I_4^{(2)}\left(\theta_{\mathrm{Fe}},\mu,T_c\right)\right]^{1/3}=0, \tag{9}$$

where

$$I_1^{(2)}\left(\theta_{\mathrm{Ba}},\theta_{\mathrm{Fe}},\mu,|W_2|\right)=\frac{\lambda_{\mathrm{Ba}}}{2}\int_{-k\theta_{\mathrm{Ba}}}^{k\theta_{\mathrm{Ba}}}\mathrm{d}\xi\frac{\sqrt{\xi+\mu}}{|\xi|+|W_2|/2}+\frac{\lambda_{\mathrm{Fe}}}{2}\int_{-k\theta_{\mathrm{Fe}}}^{k\theta_{\mathrm{Fe}}}\mathrm{d}\xi\frac{\sqrt{\xi+\mu}}{|\xi|+|W_2|/2} \tag{10}$$

$$I_2^{(2)}\left(\theta_{Fe},\mu,|W_2|\right)=\frac{4}{3}\left(\mu-k\theta_{\mathrm{Fe}}\right)^{3/2}+\int_{-k\theta_{\mathrm{Fe}}}^{k\theta_{\mathrm{Fe}}}\mathrm{d}\xi\sqrt{\xi+\mu}\left[1-\frac{\xi}{\sqrt{\xi^2+W_2^2}}\right] \tag{11}$$

$$\begin{aligned}I_1^{(3)}\left(\theta_{\mathrm{Ba}},\theta_{\mathrm{Fe}},\theta_{\mathrm{As}},\mu,|W_3|\right)=&\frac{\lambda_{\mathrm{Ba}}}{2}\int_{-k\theta_{\mathrm{Ba}}}^{k\theta_{\mathrm{Ba}}}\mathrm{d}\xi\frac{\sqrt{\xi+\mu}}{|\xi|+|W_3|/2}+\frac{\lambda_{\mathrm{Fe}}}{2}\int_{-k\theta_{\mathrm{Fe}}}^{k\theta_{\mathrm{Fe}}}\mathrm{d}\xi\frac{\sqrt{\xi+\mu}}{|\xi|+|W_3|/2}\\&+\frac{\lambda_{\mathrm{As}}}{2}\int_{-k\theta_{\mathrm{As}}}^{k\theta_{\mathrm{As}}}\mathrm{d}\xi\frac{\sqrt{\xi+\mu}}{|\xi|+|W_3|/2}\end{aligned} \tag{12}$$

$$I_2^{(3)}\left(\theta_{\mathrm{Fe}},\mu,|W_3|\right)=\frac{4}{3}\left(\mu-k\theta_{\mathrm{Fe}}\right)^{3/2}+\int_{-k\theta_{\mathrm{Fe}}}^{k\theta_{\mathrm{Fe}}}\mathrm{d}\xi\sqrt{\xi+\mu}\left[1-\frac{\xi}{\sqrt{\xi^2+W_3^2}}\right] \tag{13}$$

$$\begin{aligned}I_3^{(2)}\left(\theta_{\mathrm{Ba}},\theta_{\mathrm{Fe}},\mu,T_c\right)=&\frac{\lambda_{\mathrm{Ba}}}{2}\int_{-k\theta_{\mathrm{Ba}}}^{k\theta_{\mathrm{Ba}}}\mathrm{d}\xi\frac{\sqrt{\xi+\mu}\tanh\left(\xi/2kT_c\right)}{\xi}\\&+\frac{\lambda_{\mathrm{Fe}}}{2}\int_{-k\theta_{\mathrm{Fe}}}^{k\theta_{\mathrm{Fe}}}\mathrm{d}\xi\frac{\sqrt{\xi+\mu}\tanh\left(\xi/2kT_c\right)}{\xi},\end{aligned} \tag{14}$$

and

$$I_4^{(2)}\left(\theta_{\mathrm{Fe}},\mu,T_c\right)=\int_{-\mu}^{k\theta_{\mathrm{Fe}}}\mathrm{d}\xi\sqrt{\xi+\mu}\left[1-\tanh\left(\xi/2kT_c\right)\right]. \tag{15}$$

In the above equations, the superscripts of $I_{1,2}^{(2)}$ and $I_{1,2}^{(3)}$, for example, denote that the expressions for them correspond to 2PEM and 3PEM scenarios, respectively. Further, among the Debye temperatures of the ion-species that contribute to each of Equations (7)-(9), the value chosen in the second term is the one that has the greatest value (*i.e.*, θ_{Fe}) because a lower value would curtail the region of pairing due to one or the other species of ions. For later reference, we note that the equation for T_c corresponding to the vanishing of W_3 is obtained by replacing $I_3^{(2)}\left(\theta_{\mathrm{Ba}},\theta_{\mathrm{Fe}},\mu,T_c\right)$ in Equation (9) by $I_3^{(3)}\left(\theta_{\mathrm{Ba}},\theta_{\mathrm{Fe}},\theta_{\mathrm{As}},\mu,T_c\right)$:

$$\begin{aligned}I_3^{(3)}\left(\theta_{\mathrm{Ba}},\theta_{\mathrm{Fe}},\mu,T_c\right)=&\frac{\lambda_{\mathrm{Ba}}}{2}\int_{-k\theta_{\mathrm{Ba}}}^{k\theta_{\mathrm{Ba}}}\mathrm{d}\xi\frac{\sqrt{\xi+\mu}\tanh\left(\xi/2kT_c\right)}{\xi}\\&+\frac{\lambda_{\mathrm{Fe}}}{2}\int_{-k\theta_{\mathrm{Fe}}}^{k\theta_{\mathrm{Fe}}}\mathrm{d}\xi\frac{\sqrt{\xi+\mu}\tanh\left(\xi/2kT_c\right)}{\xi}\\&+\frac{\lambda_{As}}{2}\int_{-k\theta_{\mathrm{As}}}^{k\theta_{\mathrm{As}}}\mathrm{d}\xi\frac{\sqrt{\xi+\mu}\tanh\left(\xi/2kT_c\right)}{\xi}.\end{aligned} \tag{16}$$

For $\mu\gg k\theta_{\mathrm{BaAs}}$, the solutions of Equations (7)-(9) must agree with those of

Equations (9)-(11). This requirement is satisfied because on solving the former equations for $\mu = 100k\theta_{BaAs}$ and inputs from the set of Equations (1) and (2) (with $|W_2|$ replaced by 6.2 meV) we are led precisely to the solutions given in Equations (6). We may therefore employ Equations (7)-(9) for any value of $\mu \geq k\theta_{BaAs}$. The next step in our study is to solve these equations for different values of μ in an appropriate range.

4.5. Solutions of the μ-Incorporated GBCSEs

For some select values of μ in the range $100 \geq \mu/(k\theta_{BaAs}) \geq 1.5$ and inputs from the sets of Equations (1) and (2), we have given in **Table 1** the values of λ_{Ba}, λ_{Fe} and λ_{As} obtained via solutions of Equations (7)-(9). In accord with a basic tenet of the BCS theory, we have assumed that these λs have the same values at $T = 0$ and $T = T_c$. We also assume μ to be temperature-independent, and use it interchangeably with E_F because it has been found these differ insignificantly for the wide variety of six SCs dealt with in [24]. It is then seen that for the lowest value of μ in the range under consideration, *i.e.*, μ = 1.5 $k\theta_{BaAs}$ = 35.4 meV, Δ_1/μ = 0.175 and Δ_2/μ = 0.349. Guided by the values of these parameters obtained via a

Table 1. Values of λ_{Ba}, λ_{Fe}, and λ_{As} calculated via Equations (7)-(9) with inputs from Equations ((1) and (2)) and different assumed values of $\mu/k\theta_{BaAs}$. y is obtained by solving Equation (20), and j_0 via Equation (18) with additional inputs from Equation (27).

$\mu/k\theta_{BaAs}$	μ(meV)	λ_{Ba}	λ_{Fe}	λ_{As}	y	j_0 (10^7 Acm^{-2})
100	2361	0.0308	0.3826	0.2089	3.513	72.7
50	1181	0.0308	0.3826	0.2089	3.513	45.8
25	590.3	0.0308	0.3826	0.2089	3.514	28.8
10	236.1	0.0311	0.3827	0.2090	3.512	15.7
8	188.9	0.0312	0.3827	0.2090	3.513	13.5
6	141.7	0.0315	0.3828	0.2090	3.512	11.1
4	94.4	0.0327	0.3832	0.2092	3.506	8.52
2	47.2	0.0364	0.3858	0.2102	3.493	5.38
1.5	35.4	0.2391	0.3908	0.2114	3.461	4.49
1	23.6	0.0462	0.4055	0.2144	3.422	3.46
0.9	21.3	0.0533	0.4059	02151	3.423	3.23
0.8	18.9	0.0650	0.4036	0.2160	3.428	2.98
0.7	16.5	0.0842	0.3971	0.2173	3.439	2.72
0.6	14.2	0.1155	0.3838	0.2196	3.433	2.46
0.5	11.8	0.1156	0.3603	0.2256	3.429	2.18
0.4	9.44	0.2414	0.3264	0.2343	3.392	1.90
0.3	7.08	0.3699	0.2711	0.2459	3.342	1.59
0.2	4.72	0.6226	0.1682	0.2655	Not Calculated because λ_{Ba} violates Bogoliubov constraint	

crossover study [15]—see Property (viii) in Section 3—we now need to solve our equations for lower values of μ.

Upon attempting to solve Equations (7)-(9) for $\mu = k\theta_{BaAs} \approx 23.6$ meV, for example, we find that the second term on the RHS of Equation (9) becomes complex because of the factor $\sqrt{\xi+\mu}$ (the lower limit of its integration is $-k\theta_{Fe} \approx -34.4$ meV). Real solutions can therefore be obtained only by truncating the region of integration, *i.e.*, by replacing $(-k\theta_{Fe})$ by $(-\mu)$. As we progressively decrease μ to move towards the ratios noted under Property (viii), additional terms in our equations need to be truncated too. Rather than addressing this problem manually as the need arises, a one-step solution is to employ *real* values of all the terms on the RHS of Equations (10)-(15). With this proviso, our equations can be used for any value of μ in the range considered here, which is $100 \geq \mu/(k\theta_{BaAs}) \geq 0.1$. **Table 1** includes the results for values of μ down to $\mu/(k\theta_{BaAs}) = 0.2$.

The gist of our study so far is that we have shown that the experimental values of BaAs noted in the set of Equation (2) are explicable via values of $\{\mu, \lambda_{Ba}, \lambda_{Fe}, \lambda_{As}\}$ in any row of **Table 1**. To make predictions following from our approach, we must now fix the value of μ. To do so we need to appeal to another property of the SC, which we choose to be j_0. Before undertaking this task, to shed light on Properties (ii) and (viii) in Section 3, we recall that in a study of crossover without appeal to scattering length theory [25], for a hypothetical system characterized by a single interaction parameter, the contributions of the hole-hole and the electron-electron scatterings to the pairing amplitude were separated and a parameter ρ was defined as the ratio of these contributions. It was then seen that the BCS state is characterized by $\rho = 1$ and its progressively lower values signify a march towards the BEC end. Since we are now dealing with two interaction parameters, we adopt the following definition

$$\rho = \frac{\frac{\lambda_{Ba}}{2} Re\int_{-k\theta_{Ba}}^{0} d\xi \frac{\sqrt{\xi+\mu}}{|\xi|+|W_2|/2} + \frac{\lambda_{Fe}}{2} Re\int_{-k\theta_{Fe}}^{0} d\xi \frac{\sqrt{\xi+\mu}}{|\xi|+|W_2|/2}}{\frac{\lambda_{Ba}}{2}\int_{0}^{k\theta_{Ba}} d\xi \frac{\sqrt{\xi+\mu}}{|\xi|+|W_2|/2} + \frac{\lambda_{Fe}}{2}\int_{0}^{k\theta_{Fe}} d\xi \frac{\sqrt{\xi+\mu}}{|\xi|+|W_2|/2}}. \quad (17)$$

4.6. Fixing μ via the Experimental Value of j_0

Employing the basic equation for j_0, *i.e.*, $j_0 = n_s e v_0$, where n_s is number of superconducting electrons, e the electronic charge and v_0 the critical velocity of electrons (which is the velocity of CPs at which the gap vanishes), the following E_F-dependent equation has been derived in [24] via the same approach that led to GBCSEs, *i.e.*, via a BSE.

$$j_0(E_F) = A_5(\theta/y)(\gamma/v_g)^{2/3} E_F^{2/3}, \quad \left(A_5 = 7.406\times10^{-4}\ \mathrm{C\cdot eV^{-4/3}\cdot K^{1/3}}\right) \quad (18)$$

where $\theta = \theta_{BaAs}$ and γ and v_g are, respectively, the electronic specific heat constant and the gram-atomic volume of the SC and y is a dimensionless construct:

$$y = \frac{k\theta_{BaAs}}{P_0}\sqrt{\frac{2m^*}{E_F}}, \quad \left(P_0, m^* \text{ and } E_F \text{ in units of electron volt}\right) \quad (19)$$

where P_0 is the critical momentum of CPs at $T=0$ and m^* is the effective mass of an electron (we note that the value of A_5 in Equation (18) is twice its value given in [24] and is its corrected value). To determine y, unlike the equation employed in [24], we solve the following explicitly E_F-dependent equation derived in [26]:

$$1 = T\left[\lambda_{\mathrm{Ba}}, \Sigma'_{\mathrm{Ba}}, r_1 y\right] + T\left[\lambda_{\mathrm{Fe}}, \Sigma'_{\mathrm{Fe}}, r_2 y\right], \tag{20}$$

where

$$\Sigma'_{\mathrm{Ba}} = k\theta_{\mathrm{Ba}}/E_F\,,\ \Sigma'_{\mathrm{Fe}} = k\theta_{\mathrm{Fe}}/E_F\,, \tag{21}$$

$$T\left(\lambda_i, \Sigma'_i, y\right) = Re\frac{\lambda_i}{4}\int_0^1 \mathrm{d}x\left[T_1\left(\Sigma'_i, x, y\right) + T_2\left(\Sigma'_i, x, y\right)\right] \tag{22}$$

$$T_1\left(\Sigma'_i, x, y\right) = 4\left[-u_1\left(\Sigma'_i, x, y\right) - u_2\left(\Sigma'_i, x, y\right) + u_3\left(\Sigma'_i, x, y\right) + u_4\left(\Sigma'_i, x, y\right)\right] \tag{23}$$

$$T_2\left(\Sigma'_i, x, y\right) = 2\ln\left[\frac{1+u_1\left(\Sigma'_i, x, y\right)}{1-u_1\left(\Sigma'_i, x, y\right)}\frac{1+u_2\left(\Sigma'_i, x, y\right)}{1-u_2\left(\Sigma'_i, x, y\right)}\frac{1-u_3\left(\Sigma'_i, x, y\right)}{1+u_3\left(\Sigma'_i, x, y\right)}\frac{1-u_4\left(\Sigma'_i, x, y\right)}{1+u_4\left(\Sigma'_i, x, y\right)}\right] \tag{24}$$

$$u_1\left(\Sigma'_i, x, y\right) = \sqrt{1-\Sigma'_i x/y},\ u_2\left(\Sigma'_i, x, y\right) = \sqrt{1+\Sigma'_i x/y} \tag{25}$$

$$u_3\left(\Sigma'_i, x, y\right) = \sqrt{1-\Sigma'_i\left(1-x/y\right)},\ u_4\left(\Sigma'_i, x, y\right) = \sqrt{1+\Sigma'_i\left(1-x/y\right)} \tag{26}$$

and i = Ba or Fe.

Note that Re on the RHS of Equation (20) ensures that physically acceptable values of y are obtained by truncating the region of integration whenever required—just as it did for Equations (10)-(15).

Calculated via Equation (20), Table 1 includes the value of y corresponding to the values of $\{\mu, \lambda_{\mathrm{Ba}}, \lambda_{\mathrm{Fe}}\}$ in each row. To calculate j_0 we now need the values of γ and v_g, which we have taken as

$$\gamma = \frac{7.7}{5}\ \mathrm{mJ\cdot gat^{-1}\cdot K^{-2}},\ v_g = 12.162\ \mathrm{cm^3}. \tag{27}$$

The value of γ above is one-fifth its value given in [21] because 1 mol of BaAs = 5 gat, and v_g has been calculated by using the crystallographic data of the SC, a = 3.91 Å, c = 13.21 Å [27], its molecular mass (M) and the knowledge that there are two formula units in its unit cell, whence we are led to density (d) as 5.913 g $\mathrm{cm^{-3}}$, and to v_g via M/5d.

Calculated via Equation (18), Table 1 includes the values of j_0 corresponding to the values of μ, λ_{Ba}, λ_{Fe}, and y in each row of it. Hence, appealing to the estimated value of j_0, *i.e.*, 2.5×10^7 $\mathrm{Acm^{-2}}$ (noted under Property (ix) in Section 3), we have for BaAs the result that

$$\mu = E_F = 14.2\ \mathrm{meV}. \tag{28}$$

5. Implications of E_F = 14.2 meV for the Properties of BaAs Noted in Section 3

We have so far shown that, when E_F = 14.2 meV, the values of the smaller gap and T_c in the set of Equation (2) are explicable, symbolically, via $\{\theta_{\mathrm{Ba}}, \lambda_{\mathrm{Ba}}\}$ + $\{\theta_{\mathrm{Fe}}, \lambda_{\mathrm{Fe}}\}$ in the 2PEM scenario, and the value of larger gap via $\{\theta_{\mathrm{Ba}}, \lambda_{\mathrm{Ba}}\}$ + $\{\theta_{\mathrm{Fe}}, \lambda_{\mathrm{Fe}}\}$ + $\{\theta_{\mathrm{As}}, \lambda_{\mathrm{As}}\}$ in the 3PEM scenario. Some of the results that immediately follow from

this value of E_F are:

(a) $E_F/kT_c = 4.44$, which agrees with the value noted under Property (x).

(b) In the 1PEM scenario, the sub-set $\{\theta_{Ba}, \lambda_{Ba}\}$ leads to $|W_1| = 3.59 \times 10^{-6}$ eV, which is in accord with Property (vi).

(c) In the 2PEM scenario, sub-sets $\{\theta_{Fe}, \lambda_{Fe}\} + \{\theta_{As}, \lambda_{As}\}$ lead to $|W_2| = 9.08$ meV, which is very close to the values reported in more than one paper, as noted under Property (vii).

(d) Calculated in the 3PEM scenario via Equation (9)—with LHS replaced by Equation (16)—the values of $\{\theta_{Ba}, \lambda_{Ba}\} + \{\theta_{Fe}, \lambda_{Fe}\} + \{\theta_{As}, \lambda_{As}\}$ lead to $T_c = 51.2$, in accord with Property (iv).

With E_F fixed, we can calculate ρ vide Equation (17), and s (*i.e.*, m^*/m_e), n_s, the density of superconducting electrons, and v_0, the critical velocity of CPs, via the following equations [24]:

$$s(E_F) = A_1(\gamma/v_g)^{2/3} E_F^{-1/3} \left(A_1 \simeq 3.305\times10^{-10}\,\mathrm{eV}^{-1/3}\cdot\mathrm{cm}^2\cdot\mathrm{K}^{4/3}\right) \tag{29}$$

$$n_s(E_F) = A_2(\gamma/v_g)E_F \quad \left(A_2 \simeq 2.729\times10^{7}\,\mathrm{eV}^{-2}\cdot\mathrm{K}^2\right) \tag{30}$$

$$v_0(E_F) = A_4(\theta/y)(\gamma/v_g)^{-1/3} E_F^{-1/3} \quad \left(A_4 \simeq 1.406\times10^{8}\ \mathrm{eV}^{2/3}\cdot\mathrm{sec}^{-1}\cdot\mathrm{K}^{-5/3}\right). \tag{31}$$

With s also fixed, we can calculate the coherence length ξ via

$$\xi = \frac{\hbar v_F}{\pi\Delta} = \frac{\hbar c\sqrt{2E_F/m^*}}{\pi\Delta} \quad \left(m^* = sm_e\right). \tag{32}$$

Before we report the values of these parameters for μ = 14.2 meV, we note that—corresponding to 2361 ≤ μ ≤ 7.08 meV, as in **Table 1**—they vary as follows:

$$\begin{gathered} 0.995 \geq \rho \geq 0.240,\ 14.71 \geq s \geq 2.12,\ 5.09\times10^{22} \geq n_s \geq 1.53\times10^{20}\ (\mathrm{cm}^{-3}), \\ 64.2\times10^{4} \geq v \geq 8.9\times10^{4}\ (\mathrm{cm/sec}),\ 212 \geq \xi \geq 4.4\ (\text{Å}). \end{gathered} \tag{33}$$

For μ = 14.2 meV, the values of the above parameters are:

$$\begin{gathered} \rho = 0.420,\ s = 11.68,\ n_s = 3.06\times10^{20}\left(\mathrm{cm}^{-3}\right), \\ v_0 = 50.1\times10^{4}\left(\mathrm{cm/sec}\right),\ \xi = 7\left(\text{Å}\right) \end{gathered} \tag{34}$$

Note that: (a) the product of n_s and v_0 from Equations (33) and the electronic charge leads to $j_0 = 2.46 \times 10^7$ Acm^{-2}, in agreement with its estimated value noted as Property (ix), (b) the value of ρ in Equation (40) is in accord with Property (ii); it also signifies that BaAs is nearly in the middle of crossover regime even though we now have $\Delta_1/E_F = 0.44$ and $\Delta_2/E_F = 0.84$. The differences between these values and those noted in Property (viii) could well be because our value of E_F is based also on j_0 of the SC, and (c) s and ξ above are in the same ballpark of values as were noted under Properties (xi) and (xii), respectively.

6. Discussion

1) A key step of our approach is the "resolution" of θ_{BaAs} into θ_{Ba}, θ_{Fe} and θ_{As}. We draw attention in this connection to a paper by Kwei and Lawson [28] where,

based on neutron powder diffraction experiments, it has been reported that constituents of La_2CuO_4 do indeed have different Debye temperatures.

2) Dictated by the need to avoid complex-valued solutions, truncation of some of the integrals is another key step of our study. To makes this step physically plausible, let us consider a convoy passing through a range of mountains. As the road twists and turns through a series of valleys and hill-tops, the sunlight it receives will vary from a maximum at the highest point of the range to a minimum determined by its overall topography. Streams of itinerant conduction electrons on the 3-d Fermi surface of an SC in the backdrop of various ion species are akin to such a convoy: there will be places where the available range of phonon energies for pairing from one or the other species of ions is depleted. Recent experimental work of Tacon *et al.* [29] dealing with $YBa_2Cu_3O_{6.6}$ lends credence to this view.

3) Our considerations so far have been based on the Debye temperatures of various ions as noted in the set of Equation (1). In view of the analogy given above, we now report our findings based on a different set, which too follows from $\theta_{BaAs} = 274$ K by considering the layered structure of the SC [22]:

$$\theta_{Ba} = 326.21\ \text{K}, \theta_{As} = 172.08\ \text{K}, \theta_{Fe} = 375.92\ \text{K}\ (\theta_{BaAs} = 274\ \text{K}) \tag{35}$$

Assuming that the smaller gap is due to phonon exchanges with the Ba and As ions, we now need to fine tune it to 6.35 meV in order that all the λ values satisfy the Bogoliubov constraint for any μ in the range $100 \geq \mu/k\theta_{BaAs} \geq 0.1$. For $\mu/k\theta_{BaAs} = 0.6$, we obtain

$$\{\lambda_{Ba}, \lambda_{As}, \lambda_{Fe}\} = \{0.4810,\ 0.0110,\ 0.1480\}. \tag{36}$$

Then, with $E_F/kT_c = 4.45$, some of our results are:

(a) $y = 3.366, \rho = 0.62, \xi = 6.82$ Å, $j_0 = 2.50 \times 10^7\ \text{A} \cdot \text{cm}^{-2}$.

(b) In the 1PEM scenario, $\{\theta_{Ba}, \lambda_{Ba}\}$ values lead to $|W_1| = 5.9$ meV and $\{\theta_{As}, \lambda_{As}\}$ to $|W_1| \approx 0$.

(c) In the 2PEM scenario, $\{\theta_{Fe}, \lambda_{Fe}\} + \{\theta_{As}, \lambda_{As}\}$ values lead to $|W_2| = 9.0$ meV.

(d) In the 3PEM scenario, $\{\theta_{Ba}, \lambda_{Ba}\} + \{\theta_{Fe}, \lambda_{Fe}\} + \{\theta_{As}, \lambda_{As}\}$ values lead to $T_c = 52.7$ K.

4) From our findings based on $T_c = 37$ K and the two sets of values of $\{\theta_{Ba}, \theta_{Fe}, \theta_{As}\}$ derived from θ_{BaAs} and the facts that (a) T_c of the SC can vary between 36 and 38 K and (b) θ_{BaAs} also leads to additional values for the set $\{\theta_{Ba}, \theta_{Fe}, \theta_{As}\}$ as given in [22], it follows that GBCSEs can shed light on the multitude of Δs that have been reported for this SC; see also [30] in this connection where multiple gaps of La_2CuO_4 have similarly been dealt with. We are not aware if this feature of multi-gap SCs has been addressed via any other approach.

5) We now deal with the feature of the dome-like structure exhibited by BaAs that was noted as Property (xiii) in Section 3. To address this feature, we refer to the row corresponding to $\mu/k\theta_{BaAs} = 0.6$ in **Table 1** where $\lambda_{Ba} = 0.1155$ and $\lambda_{Fe} = 0.3838$. Considering the analogy given above, if we assume that as μ fluctuates in the range $0.9 \geq \mu/k\theta_{BaAs} \geq 0.3$ the values of λ_{Fe} change as given in **Table 1** (*i.e.*, by employing λ_{Fe} as the tuning variable), but λ_{Ba} remains frozen at 0.1155, then the values of T_c calculated vide Equation (9) yield the plot given in **Figure 1**.

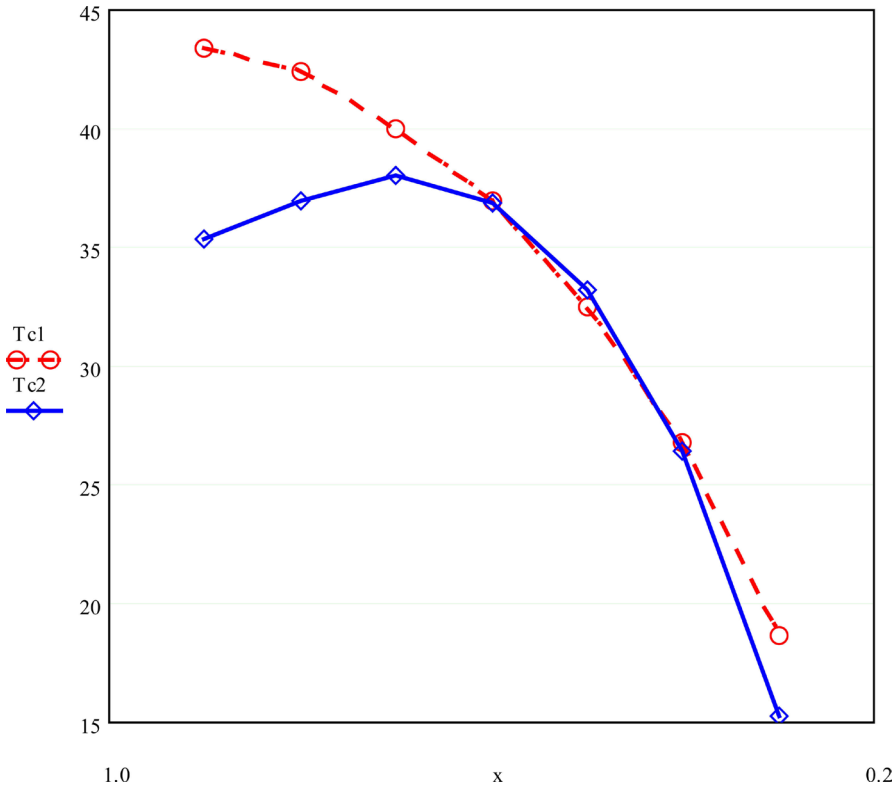

Figure 1. Plot of T_c vs. x $\equiv \mu/k\theta_{BaAs}$ for $0.9 \le x \le 0.3$ obtained by solving Equation (7) for pairing via the Ba and the Fe ions by employing values of λ_{Fe} as in **Table 1** and keeping λ_{Ba} fixed at its value corresponding to $\mu/k\theta_{BaAs} = 0.6$ (dashed curve). The solid curve is for pairing via the Ba and the As ions with a fixed value of λ_{As} (corresponding to $\mu/k\theta_{BaAs} = 0.6$), but different values of λ_{Ba}.

Given also in this figure is a similar plot when pairing is assumed to take place via the Ba and the As ions, and λ_{As} is kept fixed at its value corresponding to $\mu/k\theta_{BaAs} = 0.6$, but λ_{Ba} is varied.

7. Conclusions

1) We have shown that the values of Δs, T_c and j_0 of BaAs are correlated via the values of λ_{Ba}, λ_{Fe} and λ_{As} that the μ-incorporated GBCSEs lead to. To shed light on various other properties of the SC noted in Section 3, we needed to fix the value of μ. We were guided in this task by a crossover study of the SC. This however is not an essential step of our approach because we could, alternatively, have fixed μ by invoking Property (x).

2) We have shown that E_F plays a fundamental role in determining the Δs, T_c, j_0, m^*, v_0, n_s, ρ, and ξ of an SC. Since j_0 is not an intrinsic property of SCs, our work suggests that by varying μ in an appropriate range and using as input the θ, Δs and T_c values of different SCs, construction of a table of values of j_0, m^*, v_0, n_s, ρ, and ξ for each of them would be handy. Appeal to the experimental value of j_0 can then fix the values of μ and other parameters of the SC and may yield plausible clues about how its j_0 (and hence T_c [24]) may be enhanced.

3) In so far as the truncation of the BCS equations was also needed while

dealing with the heavy-fermion SCs [31] for which it is known that $\mu < k\theta$, it follows that GBCSEs provide a common canopy for both high-T_c SCs and the so-called exotic or unconventional SCs.

4) In the context of the yet unresolved issue of the mechanism of pairing in composite SCs, we should like to draw attention to the fact that GBCSEs imply that more than one mechanism may be at work in any such SC. To elaborate, in the 2PEM scenario, for example, GBCSEs invoke two interaction parameters, $\lambda_1 = \left[N(0)V_1\right]$ and $\lambda_2 = \left[N(0)V_2\right]$. For the sake of generality, one may assume that the interaction energies between electrons bound as CPs, V_1 and V_2, are given by $V_1 = V_{10} + U_1$ and $V_2 = V_{20} + U_2$, where V_{10} and V_{20} are the usual phononic BCS interaction terms due to the two ion-species and U_1 and U_2 are terms that depend upon the specifics of the constituents of the SC. If $U_1 = U_2 = 0$, then of course we have superconductivity caused only by phonons. If not, even when only one of the U's has non-zero value, we have a situation where the glue provided for the formation of CPs is provided by more than one mechanism.

We conclude by noting that the derivations of most of the equations employed in this paper and the concepts on which they are based, e.g., multiple Debye temperatures, superpropagator, and the Bogoliubov constraint, can be found at one place in [23].

Acknowledgements

The author thanks Professor D.C. Mattis for correspondence which led him to the approach he has followed in this and some of his earlier papers. He also thanks Professor M. de Llano and Mr. I. Chavez for drawing his attention to [15].

References

[1] Kamihara, Y., Watanabe, T., Hirano, M. and Hosono, H. (2008) Iron-Based Layered Superconductor La[$O_{1-x}F_x$]FeAs (x = 0.05–0.12) with T_c = 26 K, *Journal of the American Chemical Society*, **130**, 3296-3297. https://doi.org/10.1021/ja800073m

[2] Bang, Y. and Stewart, G.R. (2017) Superconducting Properties of the $s^{\pm}$-Wave State: Fe-Based Superconductors. *Journal of Physics: Condensed Matter*, **29**, 46. https://doi.org/10.1088/1361-648X/aa564b

[3] Suhl, H., Matthias, B.T. and Walker, L.R. (1959) Bardeen-Cooper-Schrieffer Theory in the case of Overlapping Bands. *Physical Review Letters*, **3**, 552-554. https://doi.org/10.1103/PhysRevLett.3.552

[4] Malik, G.P. and Malik, U. (2003) High-T_c Superconductivity via Superpropagators. *Physica B*, **336**, 349-352. https://doi.org/10.1016/S0921-4526(03)00302-8

[5] Malik, G.P. (2010) On the Equivalence of the Binding Energy of a Cooper Pair and the BCS Energy Gap: A Framework for Dealing with Composite Superconductors. *International Journal of Modern Physics B*, **9**, 1159-1172. https://doi.org/10.1142/S0217979210055408

[6] McMillan, W.L. (1968) Transition Temperature of Strong-Coupled Superconductors. *Physical Review*, **167**, 331-344. https://doi.org/10.1103/PhysRev.167.331

[7] Shan, L., *et al.* (2011) Observation of Ordered Vortices with Andreev Bound States in $Ba_{0.6}K_{0.4}Fe_2As_2$. *Nature Physics*, **7**, 325-331. https://doi.org/10.1038/nphys1908

[8] Li, L.-J., *et al.* (2008) Superconductivity above 50 K in $Tb_{1-x}Th_xFeAsO$. *Physical Review B*, **78**, 4.

[9] Stewart, G.R. (2011) Superconductivity in Iron Compounds. *Reviews of Modern Physics*, **83**, 1589-1652. https://doi.org/10.1103/RevModPhys.83.1589

[10] Ding, H. (2008) Observation of Fermi-Surface-Dependent Nodeless Superconducting Gaps in $Ba_{0.6}K_{0.4}Fe_2As_2$. *Europhysics Letters*, **83**, 4. http://iopscience.iop.org/article/10.1209/0295-5075/83/47001/pdf https://doi.org/10.1209/0295-5075/83/47001

[11] Lee, H. (2012) Iron-Based Superconductors: Nodal Rings. *Nature Physics*, **8**, 364-365.

[12] Ren, C., Wang, Z.-S., Luo, H.-Q., Yang, H., Shan, L. and Wen, H.-H. (2008) Evidence for Two Energy Gaps in Superconducting $Ba_{0.6}K_{0.4}Fe_2As_2$ Single Crystals and the Breakdown of the Uemura Plot. *Physical Review Letters*, **101**, 4. https://doi.org/10.1103/PhysRevLett.101.257006

[13] Popovich, P., Boris, A.V., Dolgov, O.V., Golubov, A.A., Sun, D.L., Lin, C.T., *et al.* (2010) Specific Heat Measurements of Ba0.68K0.32Fe2As2 Single Crystals: Evidence for a Multiband Strong-Coupling Superconducting State. *Physical Review Letters*, **105**, 4. https://doi.org/10.1103/PhysRevLett.105.027003

[14] Zhang, Y., Yang, L.X., Chen, F., Zhou, B., Wang, X.F., Chen, X.H., *et al.* (2010) Out-of-Plane Momentum and Symmetry-Dependent Energy Gap of the Pnictide $Ba_{0.6}K_{0.4}Fe_2As_2$ Superconductor Revealed by Angle-Resolved Photoemission Spectroscopy. *Physical Review Letters*, **105**, Article ID: 117003. https://doi.org/10.1103/PhysRevLett.105.117003

[15] Guidini, A. and Perali, A. (2014) Band-Edge BCS-BEC Crossover in a Two-Band Superconductor: Physical Properties and Detection Parameters. *Superconductor Science and Technology*, **27**, 10. https://doi.org/10.1088/0953-2048/27/12/124002

[16] Weiss, J.D., Jiang, J., Polyanski, A.A. and Hellstorm, E.E. (2013) Mechanochemical Synthesis of Pnictide Compounds and Superconducting $Ba_{0.6}K_{0.4}Fe_2As_2$ Bulks with High Critical Current Density. *Superconductor Science and Technology*, **26**, Article ID: 074003. http://iopscience.iop.org/article/10.1088/0953-2048/26/7/07/074003/pdf https://doi.org/10.1088/0953-2048/26/7/074003

[17] Taen, T., Ohtake, F., Pyon, S., Tsuyoshi, T. and Kitamura, H. (2013) Critical Current Density and Vortex Dynamics in Pristine and Proton-Irradiated $Ba_{0.6}K_{0.4}Fe_2As_2$. *Superconductor Science and Technology*, **28**, Article ID: 085003. http://iopscience.iop.org/article/10.1088/0953-2048/28/8/085003/meta

[18] Ding, H., Nakayama, K., Richard, P., Souma, S., Sato, T., Takahashi, T., *et al.* (2015) Electronic Structure of Optimally doped $Ba_{0.6}K_{0.4}Fe_2As_2$: A Comprehensive Angle-Resolved Photoemission Spectroscopy Investigation. *Journal of Physics: Condensed Matter*, **23**, Article ID: 135701. http://iopscience.iop.org/article/10.1088/0953-8984/23/13/135701/pdf

[19] Ricayzen, G. (1969) The Theory of Bardeen, Cooper, and Schrieffer. In: Parks, R.D., Ed., *Superconductivity*, Marcell Dekker, Inc., New York, 51-115.

[20] Malik, G.P. and de Llano, M. (2013) Some Implications of an Alternate Equation for the BCS Energy Gap. *Journal of Modern Physics*, **4**, 6-12. https://doi.org/10.4236/jmp.2013.44A002

[21] Mu, G., Luo, H., Wang, Z., Shan, L., Ren, C., Wen, H.-H., *et al.* (2009) Low Temperature Specific Heat of the Hole-doped $Ba_{0.6}K_{0.4}Fe_2As_2$Single Crystals and Electron-Doped $SmFeAsO_{0.9}F_{0.1}$ Samples. *Physical Review B*, **79**, Article ID: 174501. https://doi.org/10.1103/PhysRevB.79.174501

[22] Malik, G.P., Chávez, I. and de Llano, M. (2013) Generalized BCS Equations and the

Iron-Pnictide Superconductors. *Journal of Modern Physics*, **4**, 474-480. https://doi.org/10.4236/jmp.2013.44067

[23] Malik, G.P. (2016) Superconductivity-a New Approach Based on the Bethe-Salpeter Equation in the Mean-Field Approximation. Series on Directions in Condensed Matter Physics, World Scientific, Singapore city.

[24] Malik, G.P. (2016) On the Role of Fermi Energy in Determining Properties of Superconductors: A Detailed Study of Two Elemental Superconductors (Sn and Pb), a Non-cuprate (MgB_2), and Three Cuprates (YBCO, Bi-2212 and Tl-2212). *Journal of Superconductivity and Novel Magnetism*, **29**, 2755-2764. https://doi.org/10.1007/s10948-016-3637-5

[25] Malik, G.P. (2014) BCS-BEC Crossover without Appeal Scattering Length Theory. *International Journal of Modern Physics B*, **28**, Article ID: 1450054. https://doi.org/10.1142/S0217979214500544

[26] Malik, G.P. (2017) A Detailed Study of the Role of Fermi Energy in Determining Properties of Superconducting NbN. *Journal of Modern Physics*, **8**, 99-109. https://doi.org/10.4236/jmp.2017.81009

[27] Rotter, M., Tegel, M. and Johrendt, D. (2008) Superconductivity at 38 K in the Iron Arsenide ($Ba_{1-x}K_xFe_2As_2$). *Physical Review Letters*, **101**, Article ID: 107006. https://doi.org/10.1103/PhysRevLett.101.107006

[28] Kwei, G.H. and Lawson, A.C. (1991) Vibrational Properties and Atomic Debye Temperatures for La2CuO4 from Neutron Powder Diffraction. *Physica C: Superconductivity*, **175**, 135-142. https://doi.org/10.1016/0921-4534(91)90244-S

[29] Tacon, M., Bosak, A., Souliou, S.M., Dellen, G., Loew, T., Heid, R., *et al.* (2014) Inelastic X-Ray Scattering in YBa2Cu3O6.6 Reveals Giant Phonon Anomalies and Elastic Central Peak Due to Charge-Density-Wave Formation. *Nature Physics*, **10**, 52-58. https://doi.org/10.1038/nphys2805

[30] Malik, G.P. and Varma, V.S. (2015) A Study of Superconducting La_2CuO_4 via Generalized BCS Equations Incorporating Chemical Potential. *World Journal of Condensed Matter Physics*, **5**, 148-159. https://doi.org/10.4236/wjcmp.2015.53017

[31] Malik, G.P. (2015) A Study of Heavy-Fermion Superconductors via BCS Equations Incorporating Chemical Potential. *Journal of Modern Physics*, **6**, 1233-1242. https://doi.org/10.4236/jmp.2015.6912